

PAPER

## Sensitivity of radiometric results for a Lambertian source to simple changes of geometry

To cite this article: Eric L Shirley 2025 *J. Opt.* **27** 035601

View the [article online](#) for updates and enhancements.

### You may also like

- [Optimal wavelength scale diffraction gratings for light trapping in solar cells](#)  
Teck Kong Chong, Jonathan Wilson, Sudha Mokkapati et al.
- [Thermodynamics of Light Extraction from Luminescent Materials](#)  
A. Lenef, A. Piquette and J. Kelso
- [AdVLP: unsupervised visible light positioning by adversarial deep learning](#)  
Luchi Hua, Yuan Zhuang, Fuqiang Gu et al.

# Sensitivity of radiometric results for a Lambertian source to simple changes of geometry

Eric L Shirley 

National Institute of Standards and Technology, Gaithersburg, MD 20899, United States of America

E-mail: [eric.shirley@nist.gov](mailto:eric.shirley@nist.gov)

Received 16 April 2024, revised 20 December 2024

Accepted for publication 17 January 2025

Published 3 February 2025



## Abstract

This work considers the effects of changes in distance, centering and tilting of optical elements on radiometric throughput. Analytical formulas for leading-order effects are compared to numerical calculations for validation purposes.

Keywords: Lambertian, misalignment, radiometry, throughput, uncertainty

## 1. Introduction

Dimensional metrology can play an important role in optical radiometric measurements, because of the configuration factors or throughputs of optical systems. For instance, whereas measurements (before the 2019 revision of the SI) of the Stefan–Boltzmann constant by Quinn and Martin [1, 2] benefited from the use of electrical substitution radiometers (ESRs), the work also required accurate dimensional metrology. Obviously, ESRs continue to serve as longstanding, primary standards in absolute radiometric power measurements because of their intrinsically calibrated, native scales [3–5]. Practical dissemination of ESR scales, though, often relies on more practical transfer standards, such as trap detectors. In this way, absolute measurements of irradiance, radiance, radiance temperature and aperture area [6–10] have been carried out, and all this requires use of precision apertures and accurate distance measurements.

The following scenario arises in many radiometric measurements related to the above-mentioned body of work: a circular, Lambertian source is presented to a circular detector, such that the areas of these two optics and their separation determine the throughput of a system. The ‘source’ may not be the actual radiation source but might be, say, a view-limiting aperture placed in front of a blackbody cavity or integrating sphere. Similarly, the ‘detector’ might be, say, a defining aperture placed in front of an underfilled photodiode or

active cavity radiometer. In the simplest—and typical—cases, the two optics are centered on an optic axis that is an axis of cylindrical symmetry, with both optics’ surface normals parallel to the optic axis. This arrangement is illustrated in figure 1. The figure also indicates three types of misalignments or changes amounting to changes in the separation and tilt of the optics. In some instances cited above, it was necessary to deduce aperture areas radiometrically, and deviations of aperture edge locations from ideal planarity also needed to be considered.

It is the purpose of this work to provide simple formulas for the sensitivity of the throughput to these and other changes. One can use knowledge of such sensitivity to establish relationships between throughputs of similar optical systems relating using Taylor-expansion concepts and in evaluating components of uncertainty budgets owed to ambiguities about geometrical aspects of optics. The small changes may be of interest for a variety of reasons. For instance, apertures might be slightly tilted on purpose to prevent different optics having parallel surfaces that give rise to inter-reflections. Situations also arise where apertures are mounted on mechanized filter wheels or translation stages. Imperfect positioning prevents an aperture being centered on the optic axis, thereby affecting measurements. Furthermore, despite its conceptual simplicity, the distance between optics—which lies at the heart of the ‘inverse-square law’ impacting throughput—needs to be measured accurately.

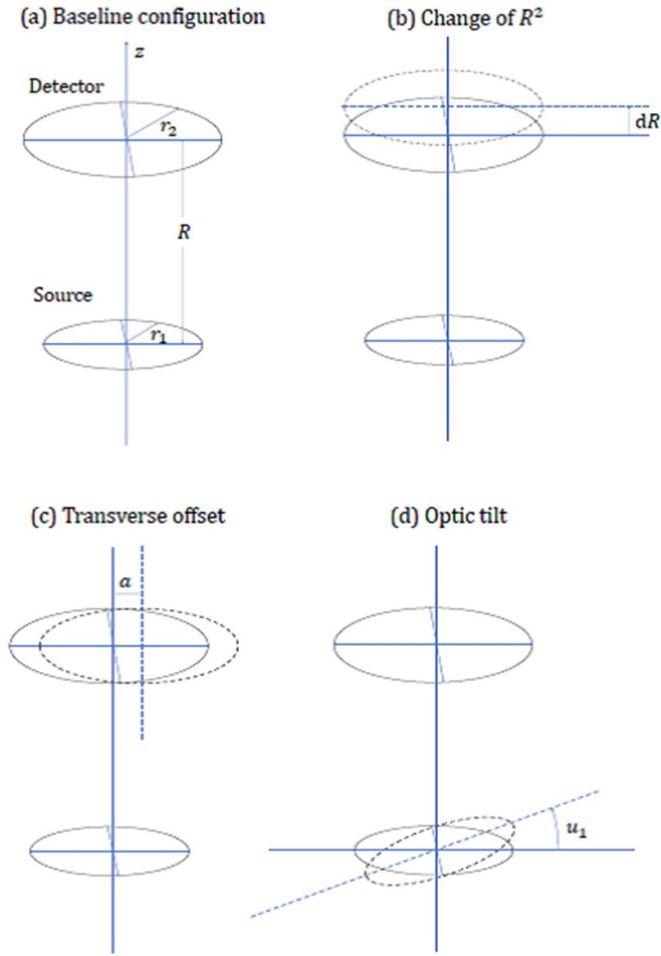


**Figure 1.** Optical configuration discussed in the text (a), and several changes thereto (b)–(d).

Section 2 derives a formula that streamlines the determination of the effects of changes on throughput. Section 3 applies the methodology derived in section 2 to obtain analytical formulas for leading-order effects of misalignments. In section 4, the effects of changes as found using the formulas and numerical calculations are compared for validation purposes.

## 2. General determination of throughput

Consider a Lambertian source with area  $A_1$  and a detector with area  $A_2$ . The flux passing through  $A_2$  is the radiance of the source times the throughput. The throughput is found by summing (integrating) over rays from each projected area element  $dA_1$  into each solid angle element,  $d\Omega_2$ , subtended by area element,  $dA_2$ . Such a solid angle element is the ratio of a projected area element  $dA_2$  to the square of the distance between  $dA_1$  and  $dA_2$ . In general, the throughput is given as  $T_{12}$  sr, with

$$\begin{aligned}
 T_{12} &= \int_{A_1} dA_1 \int_{\Omega_2} d\Omega_2 \mathbf{n}_1 \cdot \widehat{\Omega}_2 \text{ sr}^{-1} \\
 &= \int_{A_1} dA_1 \int_{A_2} dA_2 \frac{(\mathbf{n}_1 \cdot \hat{\mathbf{s}})(\mathbf{n}_2 \cdot \hat{\mathbf{s}})}{s^2} \\
 &= \int_{A_1} dA_1 \int_{A_2} dA_2 \frac{(\mathbf{n}_1 \cdot \mathbf{s})(\mathbf{n}_2 \cdot \mathbf{s})}{s^4}. \quad (1)
 \end{aligned}$$

Here  $\mathbf{n}_1$  and  $\mathbf{n}_2$  are the outward-pointing and inward-point normals on the two surfaces, respectively, and  $\mathbf{s}$  is the vector from  $dA_1$  to  $dA_2$  [11]. Note that  $dA_2$  is an actual area element. The projected area, which is subtended by  $d\Omega_2$ , includes the cosine factor,  $\mathbf{n}_2 \cdot \hat{\mathbf{s}}$ . Strictly speaking, the dimensionality of  $T_{12}$  is area, whereas the dimensionality of throughput,  $T_{12}$  sr, is area times steradian. The cosine factor,  $\mathbf{n}_1 \cdot \widehat{\Omega}_2 = \mathbf{n}_1 \cdot \hat{\mathbf{s}}$ , is a consequence of the source's Lambertian properties, as if flux passing through  $dA_1$  had been incident on the area element equally from all directions from within a half-space on the other side of the source surface plane.

When performing throughput calculations, one can often use Green's theorem to replace double integration on an area with single integration along the perimeter of the area [12]. Here, a similarly helpful device can be implemented by distorting the flat area of the detector into the surface of a semi-infinite cylinder that is parallel to the optic axis and has the same projection on the source plane as the detector area perimeter. In this sense, although the surface area of the detector is thereby distorted, its perimeter remains unchanged. The surface normal on the cylinder is parallel to the source plane everywhere except for a cap at infinite distance from the source plane. In the limit that the cylinder's length approaches infinity, the solid angle that the cap subtends anywhere on the source vanishes. Figure 2 illustrates the distortion and several variables that are relevant in what follows. The figure also shows how elements of a line integral about the true perimeter have a one-to-one correspondence with semi-infinite ribbons running the length of the cylinder.

For rays radiating into each direction from each point on the source, flux passing through the undistorted detector area equals the flux passing *out of* the cylinder after passing through its undistorted area. Moreover, one can count negative, improper flux because of rays passing *into* the cylinder's volume through the vertical surface if one also counts the positive flux when the rays subsequently pass *out of* the cylinder's volume. Exploiting this cancellation simplifies throughput calculations.

One may define the source area as a circular disk centered at the origin. Ordinarily, the source area is normal to the optic axis, which we choose to have along the  $z$ -axis, and which passes through the center of the source. Integration over the vertical area of the cylinder can be done using cylindrical polar coordinates,  $z$  (distance from the source plane),  $\rho$  (distance from the  $z$ -axis) and  $\phi$  (azimuthal angular variable). A point on the source is denoted  $s_1$ , a point on the detector perimeter

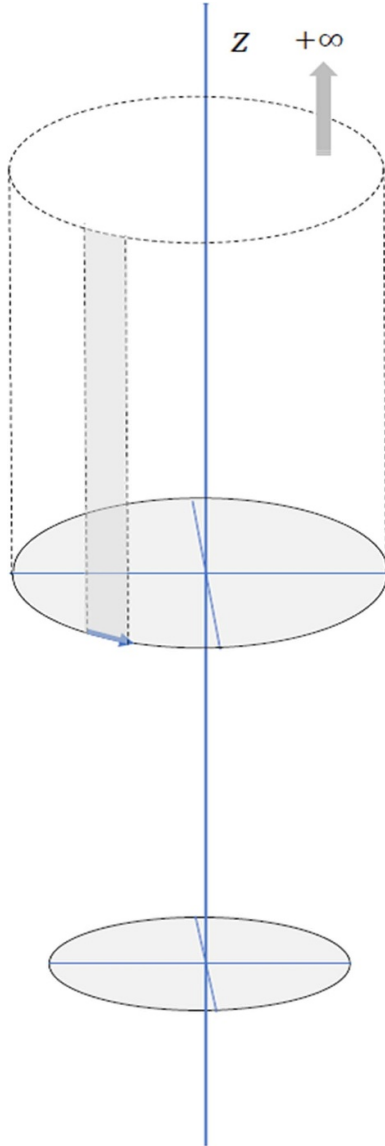


**Figure 2.** Distortion of detector surface into a cylinder.

is given by  $s_2(\phi) = z'(\phi)\hat{z} + \rho(\phi)\hat{\rho}$ , and we have

$$s = s_2 - s_1 = z'(\phi)\hat{z} + t, \quad (2)$$

with  $t$  being the transverse part of  $s$ .

Integration over the distorted detector area can be replaced by a line integral according to

$$\begin{aligned} T_{12} &= \int_{A_1} dA_1 \int d\phi \rho \int_{z'}^{\infty} dz'' \frac{(\mathbf{n}_1 \cdot \mathbf{s})(\mathbf{n}_2 \cdot \mathbf{s})}{s^4} \\ &= \int_{A_1} dA_1 \int d\phi \rho \int_{z'}^{\infty} dz'' \frac{z'' t \cos \psi}{(z''^2 + t^2)^2} \\ &= \frac{1}{2} \int_{A_1} dA_1 \int d\phi \frac{\rho t \cos \psi}{z'^2 + t^2} \\ &= \int d\phi \left( \frac{1}{2} \int_{A_1} dA_1 \frac{\rho t \cos \psi}{z'^2 + t^2} \right). \end{aligned} \quad (3)$$

Dependences of  $\rho, z'$  and  $t$  on  $\phi$  are suppressed. The angle  $\psi$  is given by  $\cos \psi = \mathbf{n}_2 \cdot \hat{\mathbf{t}}$ , where  $\mathbf{n}_2$  points from the cylinder interior outward. Limits of  $\phi$  integration are not specified, because the integration range (or ranges) depend on the perimeter of the detector. Integration with respect to  $\phi$  from 0 to  $2\pi$  would normally suffice. However, exceptions to this rule would include detectors with areas that are not simply connected, do not have convex perimeters, and/or do not intersect the optic axis.

Integration over  $A_1$  is equivalent to integration of  $t$  over the range  $|\rho - r_1| < t < \rho + r_1$  and  $-\Psi(t) < \psi < \Psi(t)$ . Figure 3 illustrates this. (In a later section, a tilt of the source disk is replaced by an equivalent off centering and tilt of the detector. Thus, our analysis always involves a centered, source disk normal to the  $z$ -axis. In this way, the foregoing analysis using plane geometry in the source plane retains validity.) The law of cosines implies

$$r_1^2 = \rho^2 + t^2 - 2\rho t \cos \psi \quad (4)$$

This implies

$$\begin{aligned} T &= \int d\phi \rho \int_{|\rho-r_1|}^{\rho+r_1} dt t^2 \int_0^{\Psi(t)} d\psi \frac{\cos \psi}{z'^2 + t^2} \\ &= \int d\phi \rho \int_{|\rho-r_1|}^{\rho+r_1} \frac{dt t^2}{z'^2 + t^2} \sin \Psi(t) \\ &= \int d\phi \rho \int_{|\rho-r_1|}^{\rho+r_1} \frac{dt t^2}{z'^2 + t^2} \left[ 1 - \left( \frac{\rho^2 + t^2 - r_1^2}{2\rho t} \right)^2 \right]^{1/2} \\ &= \frac{1}{2} \int d\phi \int_{|\rho-r_1|}^{\rho+r_1} \frac{dt t}{z'^2 + t^2} \left[ (2\rho t)^2 - (\rho^2 + t^2 - r_1^2)^2 \right]^{1/2}. \end{aligned} \quad (5)$$

One can factor the difference of squares of two quantities in the last result into the product of the sum and difference of the two quantities, factor that further, and regroup differently:

$$(2\rho t)^2 - (\rho^2 + t^2 - r_1^2)^2 = [(\rho + r_1)^2 - t^2] [t^2 - (\rho - r_1)^2]. \quad (6)$$

One can define  $r_> = \max(\rho, r_1)$ ,  $r_< = \min(\rho, r_1)$ ,  $\sigma = r_</r_>$ ,  $D = z'/r_>$ , and  $x$ , defined by

$$t = (1 + \sigma x) r_>. \quad (7)$$

Changing the inner variable of integration from  $t$  to  $x$  leads to

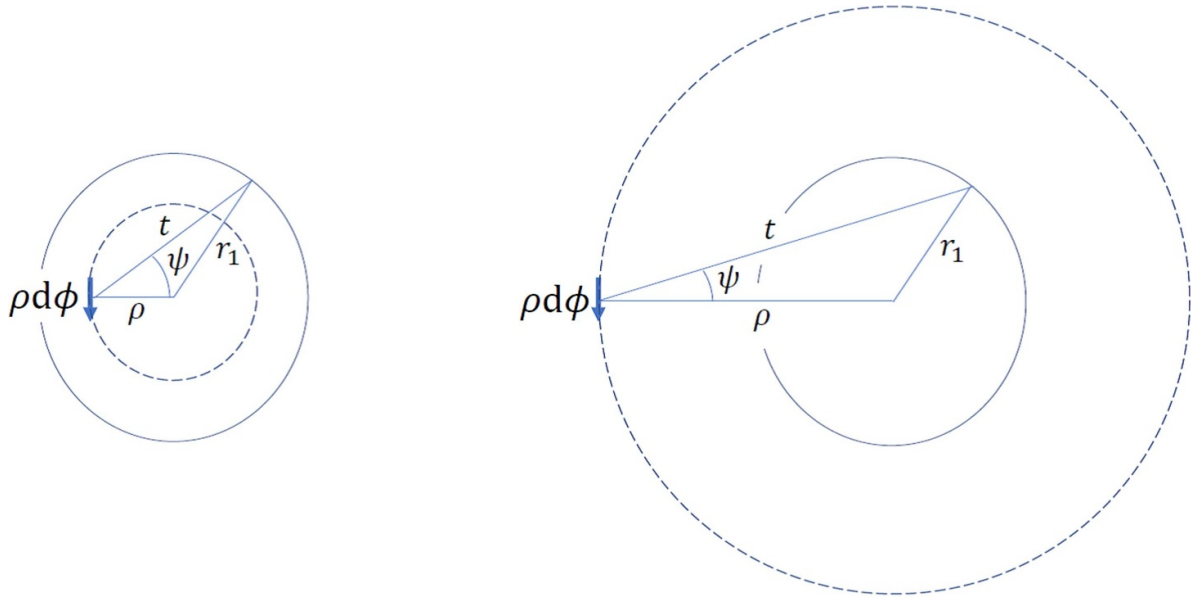


**Figure 3.** Triangles constructed to illustrate the mapping of integration over the source onto polar coordinates centered at a detector perimeter segment of length  $\rho d\phi$ . In the case on the left, one has  $\rho < r_1$ , so that  $\psi$  increases from 0 to  $\pi$  as  $t$  decreases from  $r_1 + \rho$  to  $r_1 - \rho$ . In the case on the right, one has  $\rho > r_1$ , so that  $\psi = 0$  when  $t = r_1 + \rho$  and  $t = r_1 - \rho$ , but  $\psi$  takes on non-zero values for intermediate values of  $t$ . The dashed curves indicate hypothetical projections of the detector perimeter onto the source plane.

$$T_{12} = \int d\phi \frac{r_{<} r_{>}}{2} \int_{-1}^{+1} dx (1 + \sigma x) \frac{\left\{ \left[ (1 + \sigma)^2 - (1 + \sigma x)^2 \right] \left[ (1 + \sigma x)^2 - (1 - \sigma)^2 \right] \right\}^{1/2}}{(1 + \sigma x)^2 + D^2}. \quad (8)$$

Changing the inner variable of integration, from  $x$  to

$$y = \frac{(1 + \sigma x)^2 - (1 - \sigma)^2}{2\sigma} - 1 \quad (9)$$

which gives  $dy = (1 + \sigma x) dx$ ,  $(1 + \sigma x)^2 = 1 + \sigma^2 + 2\sigma y$ , and

$$\begin{aligned} & \left[ (1 + \sigma)^2 - (1 + \sigma x)^2 \right] \left[ (1 + \sigma x)^2 - (1 - \sigma)^2 \right] \\ & = 4\sigma^2 (1 - y^2) \end{aligned} \quad (10)$$

one has [13]

$$\begin{aligned} T_{12} &= \int d\phi r_{<}^2 \int_{-1}^{+1} \frac{dy \sqrt{1 - y^2}}{1 + \sigma^2 + D^2 + 2\sigma y} \\ &= \int d\phi r_{<}^2 \left( \frac{1 + \eta^2}{1 + \sigma^2 + D^2} \right) \int_{-1}^{+1} \frac{dy \sqrt{1 - y^2}}{1 + \eta^2 + 2\eta y}. \end{aligned} \quad (11)$$

The last substitution requires

$$\left( \frac{1 + \eta^2}{1 + \sigma^2 + D^2} \right) = \frac{\eta}{\sigma} \quad (12)$$

with

$$\eta = \frac{1}{2\sigma} \left[ 1 + \sigma^2 + D^2 - \sqrt{(1 + \sigma^2 + D^2)^2 - 4\sigma^2} \right]. \quad (13)$$

The inner integral in equation (11) is  $\pi/2$ . Applying equations (12) and (13) implies

$$\begin{aligned} T_{12} &= \frac{\pi}{4} \int d\phi r_{>}^2 \left[ 1 + \sigma^2 + D^2 - \sqrt{(1 + \sigma^2 + D^2)^2 - 4\sigma^2} \right] \\ &= \frac{\pi}{4} \int d\phi \left\{ r_1^2 + \rho^2 + z'^2 - \left[ (r_1^2 + \rho^2 + z'^2)^2 - 4r_1^2 \rho^2 \right]^{1/2} \right\}. \end{aligned} \quad (14)$$

In the case of a centered, circular detector area that is normal to the optic axis, one has  $\rho = r_2$  and  $z' = R$  for all  $\phi$ . Introducing the shorthand,

$$Q_0 = \left[ (R^2 + r_1^2 + r_2^2)^2 - 4r_1^2 r_2^2 \right]^{1/2} \quad (15)$$

one obtains the classic result for the ideal throughput:

$$T_{12}^{(0)} = \frac{\pi^2}{2} \left[ R^2 + r_1^2 + r_2^2 - Q_0 \right]. \quad (16)$$

More generally, if the detector  $z'$  and  $\rho$  values vary with  $\phi$ , the throughput (given the source, which does not change) is found using one integration over  $\phi$  as indicated by equation (14).

### 3. Effects of small changes on throughput

Consider small changes in the layout in the form of  $R^2 \rightarrow R^2 + d(R^2)$ ,  $r_i^2 \rightarrow r_i^2 + d(r_i^2)$ , and the introduction of small tilts of the optics. Regarding the tilts, the outward-pointing normal of the element with radius  $r_1$  could acquire transverse direction cosines, whose leading terms are the tilt angles,  $u_1$  and  $v_1$ . Similarly, the inward-pointing normal of the element with radius  $r_2$  could acquire transverse direction cosines with leading terms  $u_2$  and  $v_2$ . These degrees of freedom form a complete set for two such optics. The modified throughput would be

$$T_{12} = T_{12}^{(0)} + \Delta T_{12} \quad (17)$$

with leading-order effects because of all small changes being

$$\begin{aligned} \Delta T_{12} = & t_R d(R^2) + t_{r_1} d(r_1^2) + t_{r_2} d(r_2^2) + t_{11} (u_1^2 + v_1^2) \\ & + t_{22} (u_2^2 + v_2^2) + t_{12} (u_1 u_2 + v_1 v_2) + \dots \end{aligned} \quad (18)$$

The author and colleagues are not aware of other presentations of the formulas for such sensitivities having been published elsewhere.

#### 3.1. Change of source-detector separation

Differentiation and rearrangement give

$$t_R = \frac{\partial T_{12}}{\partial (R^2)} = \frac{\pi^2}{2} \left( 1 - \frac{R^2 + r_1^2 + r_2^2}{Q_0} \right) = -\frac{T_{12}^{(0)}}{Q_0}. \quad (19)$$

#### 3.2. Change of source or detector size

Differentiation and rearrangement give

$$t_{r_1} = \frac{\partial T_{12}}{\partial (r_1^2)} = \frac{\pi^2}{2} \left( 1 - \frac{R^2 + r_1^2 - r_2^2}{Q_0} \right) \quad (20)$$

and

$$t_{r_2} = \frac{\partial T_{12}}{\partial (r_2^2)} = \frac{\pi^2}{2} \left( 1 - \frac{R^2 + r_2^2 - r_1^2}{Q_0} \right). \quad (21)$$

#### 3.3. Transverse offset of detector

Although it is not among the degrees of freedom mentioned above, the effect of a transverse offset of the detector on throughput may also be of interest, and knowing this effect can simplify evaluation of  $t_{12}$  if other coefficients in equation (18) are known. If the displacement is by a small amount,  $a$ , one can introduce  $t_d$  so that  $\Delta T_{12} = t_d a^2 + \dots$ . From the law of cosines, the  $\phi$ -dependent value of  $\rho$  is given through

$$\rho^2 + a^2 - 2\rho a \cos \phi = r_2^2 \quad (22)$$

implying

$$\rho = a \cos \phi + \sqrt{r_2^2 - a^2 \sin^2 \phi}. \quad (23)$$

Expanding equation (14) about  $\rho = r_2$  and isolating terms at second order in  $a$  give

$$t_d = -2\pi^2 r_1^2 r_2^2 R^2 Q_0^{-3}. \quad (24)$$

This is consistent with the ‘cosine to the fourth’ rule that becomes exact in the limit when  $r_1$  and  $r_2$  are vanishingly small compared to  $R$ . This formula is also independent of which optic is transversely displaced, which is a consequence of symmetry.

#### 3.4. Tilt of either the source or detector

Having a small  $u_1 > 0$  but  $v_1 = u_2 = v_2 = 0$  is equivalent to having the source be centered and level but having the detector be both off-center and tilted with  $\phi = \pi$  at the detector center. The center of the source is at the center of a sphere with the detector perimeter on its surface. If the sphere’s radius is  $S$ , one has  $S^2 = z'^2 + \rho^2 = R^2 + r_2^2$ , but  $z'$  and  $\rho$  vary with  $\phi$ . We also define the angles  $b$  and  $c$ , given by  $z' = S \cos b$ ,  $\rho = S \sin b$ ,  $R = S \cos c$  and  $r_2 = S \sin c$ . Thus,  $b$  is the angle subtended between a point on the detector perimeter and optical axis at the center of the source, and  $2c$  is the angle subtended by the detector at the center of the source. The spherical law of cosines ensures  $\cos c = \cos u_1 \cos b + \sin u_1 \sin b \cos(\phi - \pi) = \cos u_1 \cos b - \sin u_1 \sin b \cos \phi$ , and therefore

$$-\sin u_1 \sin b \cos \phi = \cos c - \cos u_1 \cos b. \quad (25)$$

Squaring both sides and using  $\sin^2 b = 1 - \cos^2 b$  leads to a quadratic equation in  $\cos b$ , yielding

$$\cos b = \frac{\cos u_1 \cos c \pm [\cos^2 u_1 \cos^2 c - (1 - \sin^2 u_1 \sin^2 \phi) (\cos^2 c - \sin^2 u_1 \cos^2 \phi)]^{1/2}}{1 - \sin^2 u_1 \sin^2 \phi}. \quad (26)$$

**Table 1.** Sensitivity parameter values for a configuration discussed in the text.

	Parameter			
	$T_{12}$ (mm <sup>2</sup> )	$t_R$	$t_{r_1}$	$t_{r_2}$
Numerical	37.6121	-0.003 584 71	0.372 673	0.090 4798
Formula	37.6121	-0.003 584 71	0.372 673	0.090 4798
Equation	16	19	20	21

	Parameter			
	$t_d$	$t_{11}$ (mm <sup>2</sup> rad <sup>-2</sup> )	$t_{22}$ (mm <sup>2</sup> rad <sup>-2</sup> )	$t_{12}$ (mm <sup>2</sup> rad <sup>-2</sup> )
Numerical	-0.006 835 46	-18.1294	-16.0787	1.70056
Formula	-0.006 835 46	-18.1294	-16.0787	1.70056
Equation	24	29	30	33

One can rewrite the discriminant as  $\sin^2 u_1 \cos^2 \phi (\sin^2 c - \sin^2 u_1 \sin^2 \phi)$ , which gives

$$\cos b = \frac{\cos u_1 \cos c + \sin u_1 \cos \phi \sqrt{\sin^2 c - \sin^2 u_1 \sin^2 \phi}}{1 - \sin^2 u_1 \sin^2 \phi}, \quad (27)$$

and the sign choice is now unambiguous. The quantity in square brackets in equation (14) is

$$\begin{aligned} & r_1^2 + S^2 - \sqrt{(r_1^2 + S^2)^2 - 4r_1^2 \rho^2} \\ &= r_1^2 + S^2 - \sqrt{(r_1^2 + S^2)^2 - 4r_1^2 r_2^2 - 4r_1^2 S^2 (\sin^2 b - \sin^2 c)} \\ &= r_1^2 + S^2 - \sqrt{(r_1^2 + S^2)^2 - 4r_1^2 r_2^2 + 4r_1^2 S^2 (\cos^2 b - \cos^2 c)}. \end{aligned} \quad (28)$$

Substituting equation (27) in equation (28), expanding in powers of  $\cos^2 b - \cos^2 c$ , isolating leading effects in  $u_1$  and integrating over  $\phi$  gives

$$t_{11} = -\pi^2 r_1^2 r_2^2 (R^2 + r_2^2 - r_1^2)^2 / (2Q_0^3) \quad (29)$$

and therefore also

$$t_{22} = -\pi^2 r_1^2 r_2^2 (R^2 + r_1^2 - r_2^2)^2 / (2Q_0^3). \quad (30)$$

When  $r_1$  and  $r_2$  are vanishingly small compared to  $R$ , these results imply a throughput proportional to the cosine of the tilt angle, a rule that becomes exact in such a limit.

### 3.5. Additional effects when simultaneously tilting both optics

To find  $t_{12}$ , consider the situation where one has  $u_1 = u_2 = u$  and  $v_1 = v_2 = 0$ . One has

$$\Delta T_{12} = (t_{11} + t_{22} + t_{12})u^2 + \dots \quad (31)$$

However, the situation just described is equivalent to having the combination of a relative transverse displacement given by  $a = uR$  and change in source-detector separation given by  $d(R^2) = -u^2 R^2$ , but with no tilts. The second situation gives

$$\Delta T_{12} = (t_d - t_R)R^2 u^2 + \dots \quad (32)$$

Noting this equivalence, one has

$$t_{12} = (t_d - t_R)R^2 - t_{11} - t_{22}. \quad (33)$$

## 4. Validation of results

To help validate the formulas, we chose  $R = 100$  mm,  $r_1 = 10$  mm and  $r_2 = 20$  mm. We calculated  $T_{12}$  and its derivatives numerically using five-point finite-difference formulas for required derivatives and (mixed) second derivatives by applying equation (1). Integrations were performed as four-dimensional integrals using well-converged cubature grids on both optics. A two-dimensional polar grid was used on each optic. The angular variable was regularly sampled, while the radial grid was sampled using extended Gauss-Legendre quadrature. Table 1 shows results and those obtained from analytic formulas. The numerical calculations can tolerate any amount of change, in the sense that throughput can be calculated. However, the model formulas only address the leading-order term in a series expansion of throughput versus changes of geometry. The importance of higher-order terms can best be assessed numerically and is admittedly beyond the scope of this work.

Because this work derives the first terms in a series expansion of throughput versus changes of geometry, and because this work is a purely mathematical investigation, this work is not suitable for an experimental proof-of-concept. In fact, it is expected that other effects will tend to dominate uncertainty budgets, but that bounding the effects considered in this work is a sufficient treatment of estimating their role.

## 5. Conclusions

The formulas presented for sensitivities of throughput to various small changes are summarized by equations indicated in the Table. These can be helpful for propagating uncertainties and estimating throughput in systems that are changed in known and/or intentional ways. In all of this, readers are reminded that this work only treats extended, uniform, Lambertian sources and assumes that well-characterized, uniform detectors are used.

## Data availability statement

All data that support the findings of this study are included within the article (and any supplementary files).

## Acknowledgment

The authors thank B Carol Johnson, S G Kaplan, Albert C Parr, and Ryan M Evans for helpful discussions.

## ORCID iD

Eric L Shirley  <https://orcid.org/0000-0002-0154-8647>

## References

- [1] Quinn T J and Martin J E 1984 A radiometric determination of the Stefan-Boltzmann constant *Precision Measurement and Fundamental Constants II* **617** 291
- [2] Quinn T J and Martin J E 1985 A radiometric determination of the Stefan-Boltzmann constant and thermodynamic temperatures between 240 °C and 1100 °C *Philos. Trans. R. Soc. A* **316** 85
- [3] Martin J E, Fox N P and Key P J 1985 A cryogenic radiometer for absolute radiometric measurements *Metrologia* **21** 147–55
- [4] Gentile T R, Houston J M, Hardis J E, Cromer C L and Parr A C 1996 National institute of standards and technology high-accuracy cryogenic radiometer *Appl. Opt.* **35** 1056
- [5] Houston J M and Rice J P 2006 NIST reference cryogenic radiometer designed for versatile performance *Metrologia* **43** S31
- [6] Yoon H W, Allen D W, Gibson C E, Litorja M, Saunders R D, Brown S W, Eppeldauer G P and Lykke K R 2007 Thermodynamic-temperature determinations of the Ag and Au freezing temperatures using a detector-based radiation thermometer *Appl. Opt.* **46** 2870
- [7] Smith A W, Carter A C, Lorentz S R, Jung T M and Datla R V 2003 Radiometrically deducing aperture sizes *Metrologia* **43** S13
- [8] Fowler J and Litorja M 2003 Geometric area measurements of circular apertures for radiometry at NIST *Metrologia* **40** S9
- [9] Anhalt K and Machin G 2016 Thermodynamic temperature by primary radiometry *Philos. Trans. R. Soc. A* **374** 20150041
- [10] Briaudeau S, Sadli M, Bourson F, Rougi B, Rihan A and Zondylne J-J 2011 Primary radiometry for the *mise-en-pratique*: the laser-based radiance method applied to a pyrometer *Int. J. Thermophys.* **32** 2183
- [11] Siegel R and Howell J R 2002 *Thermal Radiation Heat Transfer* 4th edn (Taylor and Francis) p 159
- [12] Ref. 11, pp. 179ff
- [13] Shirley E L 2016 Refined treatment of single-edge diffraction effects in radiometry *J. Opt. Soc. Am.* **33** 1509–22